



Preparation and Characterization of Pd-Ti Electrocatalyst on Carbon Supports for Oxygen Reduction

Y. M. Sun^{1,*}, M. Alpuche-Aviles², A. J. Bard², J. P. Zhou¹, and J. M. White²

¹Texas Materials Institute and Center for Materials Chemistry, The University of Texas at Austin, Austin, TX 78712, USA

²Department of Chemistry and Biochemistry, The University of Texas at Austin, Austin, TX 78712, USA

Nanoscale bimetallic Pd-Ti catalysts on carbon supports were prepared in liquid using ammonium tetrachloropalladate and titanium isopropoxide. The size of the metal particles ranged from sub-nanometer to greater than 10 nm, and the X-ray diffraction pattern of metal particles was dominated by a cubic crystalline structure. Depending upon the preparation conditions, the catalysts were comprised of Pd and TiO₂ or Pd₃Ti-like alloy. The surface Ti/Pd ratio was much greater than the original metal loading. We propose that the bimetallic particles were comprised of short-range Pd and TiO₂ or Pd-Ti alloy nanocrystal covered by a thin TiO₂ layer.

Keywords: Bimetallic Pd-Ti Catalyst, Nanostructure, Oxygen Reduction.

RESEARCH ARTICLE

1. INTRODUCTION

One of the principal technical challenges for fuel cell applications is to reduce the cost of fuel cell stacks by increasing the effectiveness of precious and rare metal catalysts and other stack components.^{1–3} This largely involves electrode materials and cell optimization to improve power density, durability and resistance to gas impurities. Currently, platinum (Pt) supported on high surface area carbons is the only electrocatalyst used for the cathode in proton exchange membrane fuel cell (PEMFC) systems, which have been intensively developed in recent years as an alternative power source. However, because of the high cost of Pt, much research has focused on alternative electrocatalysts, such as alloying a noble metal with a transition metal and/or a greater dispersion.^{4–6} Many studies have reported that Pt alloys with transition metals are more active for oxygen reduction reaction (ORR) than is pure Pt.^{7–9} The increase in the oxygen reduction rate was attributed to several mechanisms, such as the change in Pt–Pt bond distance,⁷ the modification of the 5-d orbital vacancies of Pt atoms,⁸ and the enhancement of active Pt site and a decrease in surface oxide.⁹ However, the dissolution of highly dispersed Pt particles during PEMFC operation makes the drastic reduction of Pt difficult. Therefore, non-Pt metal catalysts, such as organometallic complexes,¹⁰ Ru based catalyst¹¹ and Pd-Co-Mo catalysts¹² are desirable.

In previous papers, we described rapid screening methods for selecting candidate catalysts.^{13–15} Among the candidates, a Pd-Ti catalyst has shown equal or even slightly better performance than the more expensive Pt currently used for ORR in PEMFC. Screening in 0.5 M H₂SO₄ by scanning electrochemical microscopy (SECM) and subsequent electrochemical studies led to the identification of a composition with 50:50 Pd-Ti (atom %) prepared by reduction of the metal salts at a temperature of 550 °C. In this paper, we applied X-ray diffraction (XRD), X-ray photoelectron spectroscopy (XPS), scanning electron microscopy (SEM), transmission electron microscopy (TEM) and X-ray energy dispersive spectroscopy (EDS) to characterize the chemical structure of nanoscale Pd-Ti catalysts and to learn how the annealing temperature and reducing gas influence the catalyst composition and structure, which may reveal the catalytic mechanism for oxygen reduction.

2. EXPERIMENTAL DETAILS

2.1. Chemicals

Ammonium tetrachloropalladate (NH₄)₂PdCl₄ (99.995+%, Aldrich), titanium isopropoxide (Sigma-Aldrich), ethylene glycol (EM Science) were used as received. Glassy carbon plates (type II, 1 mm thick) and Vulcan carbon powder XC-72R were purchased from Alfa Aesar and Cabot Co, respectively. Glassy carbon plates were cut in 1 × 1 cm

* Author to whom correspondence should be addressed.

squares and ultrasonicated in methanol for 10 min. Solutions of titanium isopropoxide were prepared by adding aliquots of the alkoxide to ethylene glycol and quickly closing the container. The solution was vortexed and then ultrasonicated in a water bath until a clear solution was obtained (*ca.* 20 min). The solution was allowed to cool to room temperature before it was used.

2.2. Preparation of Carbon Supported Pd-Alloy Electrocatalysts

Catalyst of Pd-Ti supported on carbon black XC-72R were prepared by an impregnation method with a total metal loading of 20 wt%. Aliquots of 0.4 M solutions of ammonium tetrachloropalladate and titanium isopropoxide in ethylene glycol were added with constant stirring to a carbon slurry prepared by suspending 160 mg of Vulcan XC-72R carbon black in 150 ml of acetone. This suspension was ultrasonicated in a water bath at room temperature for 30 min. The solvent was evaporated on a hot plate. The material was placed on an alumina boat and a further dried at 180 °C in a tube furnace under Ar (1 atm). A final annealing treatment was applied to the catalyst at either 550 °C or 900 °C in Ar or H₂ (1 atm) for 1 h. For all heating treatments a 5 °C/min heating ramp was used. For XPS analysis, in addition to powder samples, thin films on glassy carbon (GC) were prepared and are designated as Ti/GC, Pd/GC and TiPd_x/GC. These samples were made from spots of 0.3 M solutions of the individual metal compounds in ethylene glycol and with suspensions of Pd/Ti ratios of 1 and 3 (from mixtures of the individual solutions). Drops of the metal suspension (2–6 μl) were deposited onto a GC plate and dried at 180 °C (Ar, 1 atm). The spots were heated under Ar or H₂ (1 atm) at 900 °C for 1 h in a tube furnace using the same treatments as for the catalysts supported on Vulcan carbon XC-72R.

2.3. Physical Characterization of Pd/Ti Catalyst

XRD data were collected at room temperature using a Bruker-AXS D8 Advance θ - 2θ powder diffractometer equipped with Cu sealed tube source and a Sol-X solid state detector. Data were collected from 20–80° in 2θ using the locked coupled scan technique at 1.5 (2.6) seconds per step for the 900 (500) °C annealed samples. The average compositions of prepared catalysts were measured by EDS attached to a LEO 1530 SEM. The high resolution micrograph and microcompositions of individual nanoparticles of the powder catalysts were analyzed on a JEOL 2010F TEM equipped with EDS in TEM mode. For XPS analysis, spectra were taken on a PHI 5700 XPS system using a monochromatic Al X-ray source operated at pass energies of 117.4 eV for surveys and 11.7 eV for high-resolution scans. The binding energy was calibrated using Au4f, Cu2p, and Ag3d.

3. RESULTS AND DISCUSSION

Figure 1 presents the powder XRD patterns of the carbon-supported Pd-Ti (1:1 ratio) catalysts annealed in H₂ at 550 °C and 900 °C, respectively. The XRD pattern for the catalyst annealed at 550 °C, spectrum (a), exhibits the characteristic peaks of crystalline Pd at $2\theta = 40.4^\circ$, 46.8° , and 68.3° , which correspond to Pd (111), (200) and (220) planes, respectively. In addition, there is a very broad peak at $2\theta = 25.5^\circ$ which matches the most intense peak of anatase TiO₂. The diffraction peak resulting from the carbon support is nearby at $\sim 24.5^\circ$. If there is any anatase TiO₂, its peak is either broader or less intense. This may explain why no other peaks of anatase TiO₂ appear in the spectrum. The breadth of this peak indicates that the major portion of the TiO₂ was amorphous phase and/or nanocrystalline. The XRD patterns for Pd-Ti catalyst annealed at 900 °C exhibited additional peaks at $2\theta = 23.3$, 32.8 , 36.3 and 53.0 , spectrum (b). The three most intense peaks, compared with the previous XRD pattern for 550 °C sample, are slightly shifted to higher Bragg angle. The three major peaks and the peaks at $2\theta = 23.3$, 32.8 , 36.3 and 53.0 match the pattern of a cubic structure of Pd₃Ti alloy, but with a $\sim 0.4^\circ$ shift to lower Bragg angles. Crystalline Pd₃Ti crystal is primitive cubic, while Pd is face-centered cubic. The peak shift implies a distortion of the unit cell dimensions, which may be induced by some inhomogeneity in the Pd/Ti ratio. The difference between the two XRD patterns indicates that a major

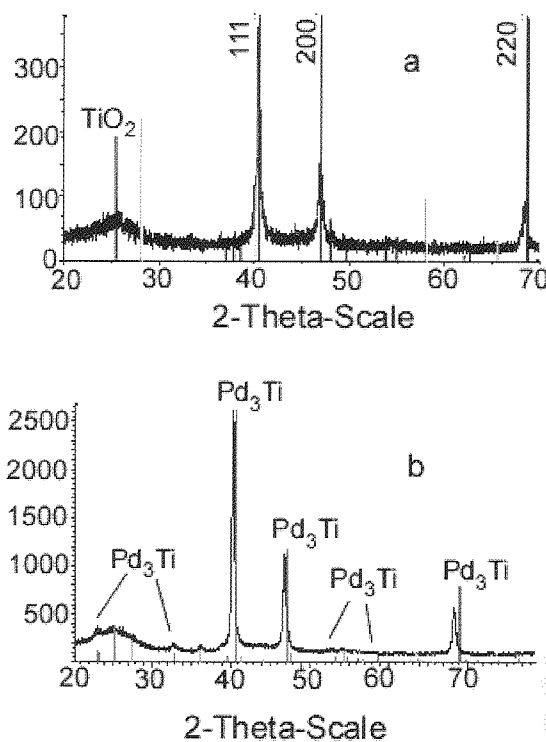


Fig. 1. XRD for Pd-Ti catalysts annealed at (a) 550 °C (b) 900 °C in H₂.

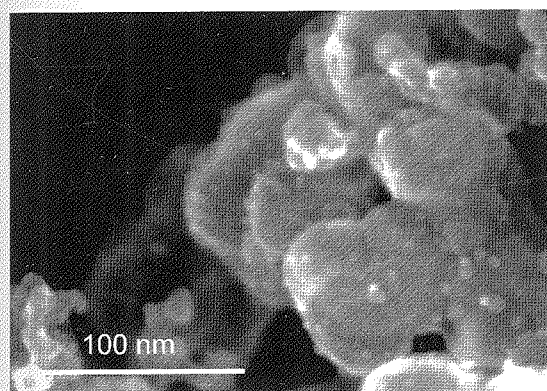


Fig. 2. SEM image for the Pd-Ti catalyst annealed at 550 °C in H₂.

change in the crystalline structure occurred at a annealing temperature above 550°C. The crystallite sizes estimated from the XRD data using Scherer's equation were 19 nm diameter for samples annealed at 900 °C and 550 °C.

Figure 2 is a high resolution SEM image for carbon-supported catalysts annealed at 550 °C. The image shows that most metal particles range from a few nanometers to greater than ten nanometers. Table I presents average compositions of areas at various magnifications, measured by EDS. For catalysts annealed at both 500 °C and 900 °C, the Ti/Pd ratios for large areas (low magnification) are close to the initial metal loading in the preparation process. The variation increased as smaller areas were selected, suggesting composition non-uniformity originating from the synthesis technique or from the subsequent heat-treatment. To further explore the composition uniformity at nanoscale level, microanalyses of selected carbon-supported Pd-Ti nanoparticles were performed by TEM-EDX. Figure 3 shows high resolution TEM micrographs of catalyst particles annealed at 900 °C. The TEM image presents some relatively large particles with diameters of 10–20 nm, and other smaller particles. The atomic compositions of eight different nanoparticles (marked in Fig. 3) are not identical, Table II. The Pd concentration for most large particles ranges from 80 to 90%. For areas without particles, EDS analysis found neither Ti nor Pd, which implies that carbon particles were not covered by Ti or Pd layers. Overall,

Table I. The composition of Pd-Ti catalysts supported on carbon-black measured by EDS.

Element	Magnification at 700×	Magnification at 1.7K×	Magnification at 9.6K×	Magnification at 5.6K×
550 °C annealed in H ₂				
Ti, %	48.8	48.8	51.6	58.8
Pd, %	51.2	51.2	48.4	41.2
Element	Magnification at 700×	Magnification at 1.6K×	Magnification at 9.6K×	Magnification at 5.6K×
900 °C annealed in H ₂				
Ti, %	47.3	48.6	52.9	43.0
Pd, %	52.7	51.4	47.1	57.0

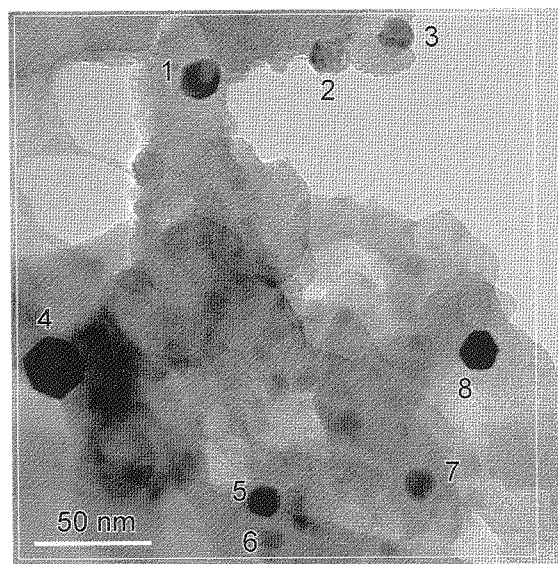


Fig. 3. TEM image for the Pd-Ti catalyst annealed at 900 °C in H₂.

more than 20 isolated nanoparticles were analyzed, with all displaying very similar compositional distribution. The average particle composition for samples annealed at 550 (900) °C is Pd 77%, Ti 23% (Pd 78%, Ti 22%), not counting the pure Ti particles. No Pd was detected for areas dominated by small particles (<5 nm). A dark field scanning TEM (STEM) image, Figure 4, confirms that the composition of individual particles is largely size dependent. The STEM not only provides high resolution images of the nanoparticles, but also presents Z contrast for these particles. This image shows many small particles with very similar size, but very different contrast. Except for a few bright particles, most of these small particles have lower contrast, indicating they are mostly Ti. This size dependence may result from a reaction stoichiometry that left some unreacted Ti salt, which became small particles when the solvent evaporated during thermal treatment and Ti oxide formed.

Besides composition analysis, single particle electron diffraction was also performed to check the crystal structure of individual particles. Figure 5 shows a diffraction pattern and a clear fringe for a Pd-rich particle composed

Table II. Composition of individual particles marked in Figure 3 measured by TEM-EDS for TiPd/carbon-black annealed at 900 °C in H₂.

Particle	Pd %	Ti %
1	78	22
2	0	100
3	84	15
4	69	31
5	82	18
6	0	100
7	75	25
8	84	16
Whole area	28	72

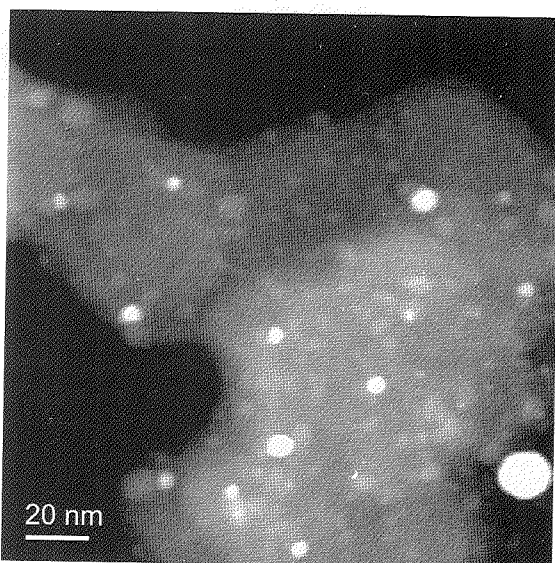


Fig. 4. Dark field STEM image for Pd-Ti Catalyst annealed at 550 °C in H₂.

of 78% Pd and 22% Ti. The cubic diffraction pattern is consistent with the XRD pattern that revealed Pd-Ti alloy with a cubic structure. In addition, a hexagonal diffraction pattern was found for a particle containing Ti but no Pd, which may correspond to Ti oxide. Of 10 particles analyzed, 7 have clear fringes for catalysts annealed at 900 °C, while only 1 have fringes for catalysts annealed at 550 °C. These results are consistent with XRD patterns where catalysts annealed at 900 °C show much more intense diffraction peaks.

Further characterization was performed by XPS. Catalysts supported on glassy carbon and carbon black and annealed at different temperatures all present very similar spectra. The peak positions of some Ti2p and Pd3d spectra

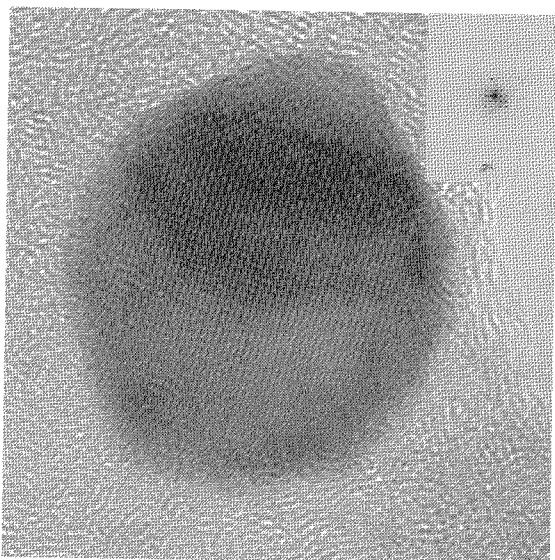


Fig. 5. High resolution TEM image and electron diffraction pattern for a Pd-Ti catalyst particle annealed at 900 °C in H₂.

Table III. The peak position of Ti2p_{3/2} and Pd3d_{5/2} for Pd-Ti catalysts.

	Pd3d _{5/2} Peak position, eV	Pd3d _{5/2} Peak width, eV
Annealed at 550 °C in H ₂ on carbon-black	335.3	1.012
Annealed at 550 °C in H ₂ on glassy carbon	335.3	0.951
Pure Pd crystal without cleaning	335.3	1.317
Pure Pd crystal	335.0	0.920
Annealed at 900 °C in H ₂ on carbon-black	335.7	1.265
	Ti2p _{3/2} Peak position, eV	Ti2p _{3/2} Peak width, eV
Annealed at 550 °C in H ₂ on carbon-black	459.4	1.079
Annealed at 550 °C in H ₂ glassy carbon	459.4	0.957
Pure TiO ₂ crystal	459.4	0.886
Annealed at 900 °C in H ₂ on carbon-black	459.4	1.059

are listed in Table III. For comparison, the XPS spectra of pure Pd, Ti and TiO₂ were also gathered. Figure 6 shows the Ti2p and Pd3d spectra for catalysts annealed at 550 °C and 900 °C under H₂, respectively. For all catalysts examined, the binding energy and line shape of Ti2p peaks match those of TiO₂.¹⁶ In contrast, neither Pd oxide (336.4 eV for PdO and 338.0 eV for PdO₂) nor pure Pd (335.0 eV) matches the binding energy of Pd3d.¹⁶ A ~0.3 eV shift of Pd3d_{5/2} to higher binding energy and the increased peak width compared to pure Pd were observed for most tested samples, except for those annealed at 900 °C, which indicates a slightly oxidized Pd surface. For a thin film sample annealed at 900 °C, a small peak at 450.2 eV appeared in the Ti2p spectrum, as well as a larger shift of 0.7 for Pd3d, which may correspond to the formation of Ti-Pd alloy. The Ti/Pd ratio in XPS for all carbon black-supported catalysts is between 2 and 6, much higher than the initial metal loading. This ratio decreased when Ar ion sputtering was applied, indicating that the particle surface may be covered with Ti layer.

Considering the ease of Ti oxide formation in air, Ar ion sputtering was applied to several thin film samples. The strongest XPS evidence for alloy formation is presented in Figure 7 for a sample having a Pd/Ti ratio of three and annealed at 900 °C in H₂. After light sputtering, spectra (b), the Ti2p profile showed a significant intensity increase at 455.2 eV. Then, after further Ar sputtering, spectra (c), the profile is very different; the major Ti2p_{3/2} peak shifted from 459.4 eV to 455.2 eV, and Ti2p_{3/2} and Ti2p_{1/2} were distinguishable. As discussed later, this depth profile spectrum is altered for samples with different thermal treatment. The Pd3d_{5/2} peak shifted to 355.8 eV, i.e., 0.8 eV higher than pure metallic Pd3d_{5/2}. Bzowski's XPS study on Pd₃Ti alloy showed that the binding energy of

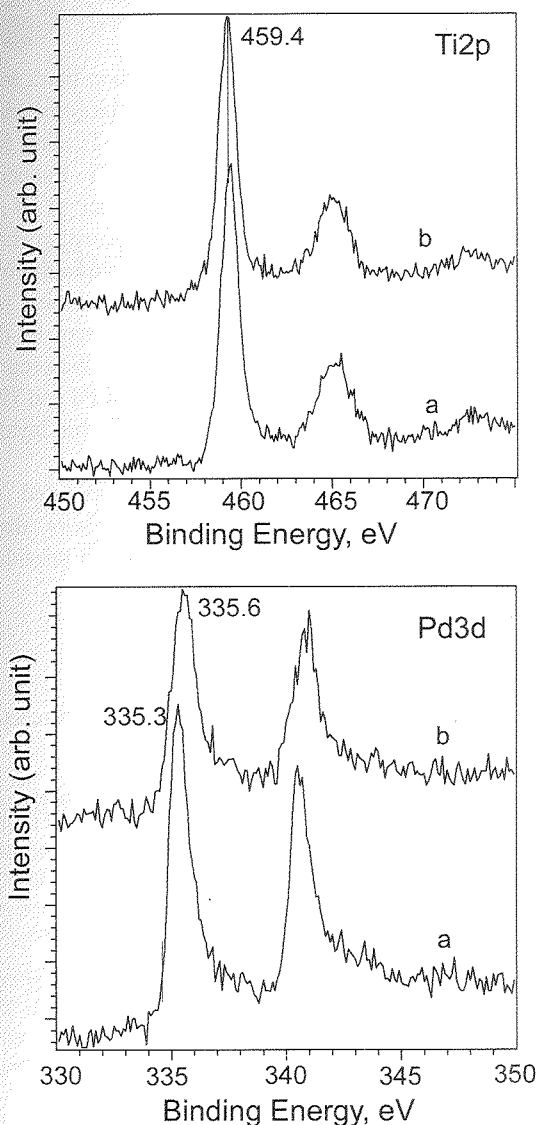


Fig. 6. Ti2p and Pd3d XPS spectra for Pd-Ti catalysts supported on carbon-black annealed at in H₂ (a) 550 °C and (b) 900 °C.

Ti2p and Pd3d both shifted 0.86 eV and 0.80 eV to the higher side,¹⁷ respectively. Compared to the value of shifts reported by Bzowski, the Pd3d is consistent with the Pd₃Ti alloy, but the shift in Ti2p is 0.35 eV larger. The larger Ti2p shift could be caused by (a) some remaining Ti oxide, and/or (b) a Pd/Ti ratio of the alloy higher than three after sputtering. The XPS measurement showed the Pd/Ti ratio reached 4.55 after three minutes sputtering, perhaps due to different sputtering yields for Ti and Pd. Since the net charge transfer is from Ti to Pd, higher Pd/Ti ratios could cause each Ti atom to lose more charge to surrounding Pd atoms, which could explain the larger shift we observed.

With this evidence for Pd-Ti alloy formation, additional tests were carried out to discern the most critical conditions for alloy formation. Substrate, the presence of Pd, annealing ambient and temperature variables were applied for verifying the Pd-Ti alloy formation. The depth profile

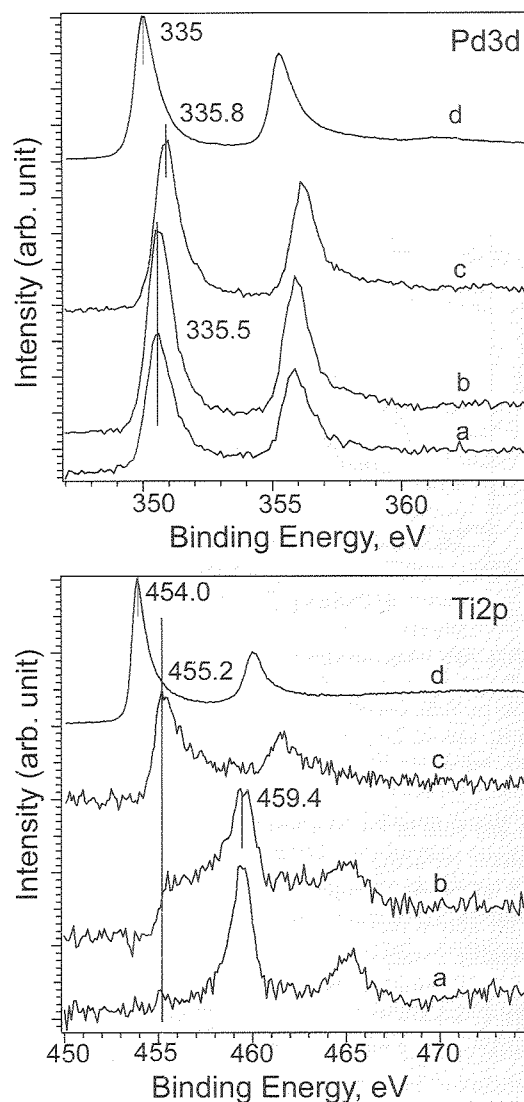


Fig. 7. Pd3d and Ti2p XPS spectra for a thin film Pd-Ti catalysts annealed at 900 °C in H₂, (a) as received (b) after Ar ion sputtering for 5 sec (c) 3 min sputtering and (d) pure Pd or Ti metal.

of the Ti2p XPS spectrum was used to qualitatively prove the existence of Pd-Ti alloy. Figure 8 shows a set of Ti2p spectra before and after Ar ion sputtering. All tested samples show an identical Ti2p spectrum, characterized as TiO₂, before sputtering. After 3 min Ar ion sputtering, these spectra show some similarity, e.g., broadening with a shift of peak onset toward lower binding energy. The initial Ti2p_{3/2} and Ti2p_{1/2} are still observed in the spectra. For comparison, the spectra of a single crystal TiO₂ sample are also presented (inset) and no qualitative difference was seen. Moreover, the Pd3d spectra also shift toward the binding energy of pure Pd and reached 335.1 eV, except for the sample annealed at 550 °C in H₂, which showed an increase of peak width and no shift towards the position of pure Pd. This fact may indicate that there was a mixture of Pd and Pd-Ti alloy, but the alloy was amorphous (no alloy diffraction pattern seen). It is clear that substrate did

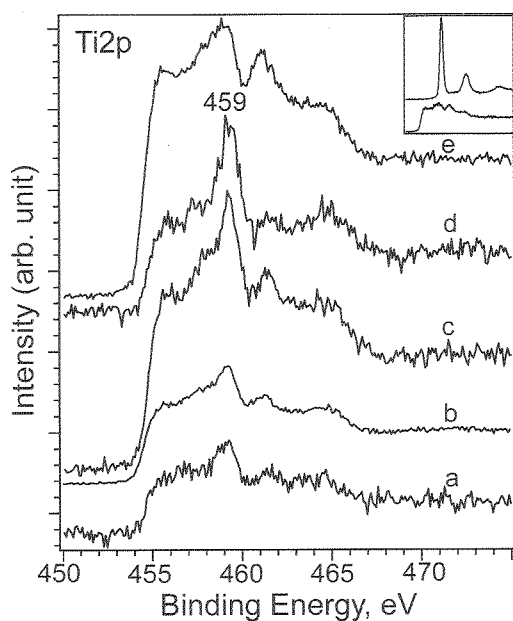


Fig. 8. Ti2p XPS taken samples after Ar ion sputtering for thin films of (a) Pd-Ti (3:1)/C, annealed 900 °C in Ar, (b) Pd-Ti (3:1)/Si, annealed 900 °C in Ar (c) Ti/Si, annealed 900 °C, in Ar, (d) Pd-Ti (1:1)/C, annealed 550 °C in H₂, and (e) Ti/C, 900 °C in H₂. The inset is XPS for a single crystal TiO₂ before and after Ar ion sputtering.

not play any role in Pd-Ti alloy formation, while annealing temperature, reducing ambient and the presence of Pd are the most influential factors.

With all above results, we propose a reaction route for the bimetallic catalysts. When two salts were mixed, the bimetallic precipitation should contain a precursor, R-O-Ti-(O-Pd-Cl_x)_y, where the number of Pd ligands depends upon the reaction control. In our case, it is likely that the majority of the precursor has 3 to 4 of the Pd ligands. Upon thermal treatment, the N and Cl components go to the gas phase, but the final chemical status of the metallic components depends upon temperature and ambient gas. Here the reduction of Ti (IV) is a key step, because TiO₂ is a very stable compound and its melting point is as high as 1800 °C. If there is no reducing gas, the Ti is transformed into TiO₂. On the other hand, Pd is a noble metal and its oxides, PdO₂ and PdO, decompose at 250 and 750 °C, respectively. Our results indicate that, in addition to high temperature and reducing gas, the presence of Pd is also critical for Ti (IV) reduction. The role of Pd in the Ti reduction process may relate to its ability to dissociate H₂, which would greatly enhance the reduction power of the individual hydrogen atoms. Therefore, depending upon the thermal treatment, the catalysts can be mainly Pd metal coupling with TiO₂, or Pd-Ti alloy coated with thin TiO₂ layer.

4. CONCLUSIONS

Nanoscale bimetallic Pd-Ti catalysts on carbon-black supports were formed when ammonium tetrachloropalladate and titanium isopropoxide were mixed. Pd₃-Ti alloy formation was verified by XRD, TEM and XPS. Reducing gas H₂, annealing temperature and the presence of Pd are the necessary conditions for Pd-Ti alloy formation. Low temperature annealing generates bimetallic particles comprised of Pd and TiO₂. A pure TiO₂ phase separation was identified by STEM and TEM-EDS, which may be due to reaction stoichiometry and process control. We propose that the bimetallic particles were comprised of Pd and TiO₂ or Pd-Ti alloy nanocrystal covered by a TiO₂ thin layer.

Acknowledgments: This work was supported by the Welch Foundation Grant F-0032. Authors thank Dr. Vincent Lynch for taking XRD spectra and providing related information.

References and Notes

1. T. He, E. Kreidler, L. Xiong, J. Luo, and C. J. Zhong, *J. Electrochem. Soc.* 153, A1637 (2006).
2. G. J. K. Acres, *J. Power Sources* 100, 60 (2001).
3. H. L. Hellmana and R. van den Hoed, *Int. J. of Hydrogen Energy* 32, 305 (2007).
4. V. Baglio, A. S. Arico, A. Stassi, C. D'Urso, A. Di Blasi, A. M. C. Luna, and V. Antonucci, *J. Power Sources* 159, 900 (2006).
5. C.-J. Tseng, S.-T. Lo, S.-C. Lo, and P. P. Chu, *Mater. Chem. Phys.* 100, 385 (2006).
6. A. Stassi, C. D'Urso, D. Baglio, A. Di Blasi, V. Antonucci, A. S. Arico, A. M. C. Luna, A. Bonesi, and W. E. Triaca, *J. Appl. Electrochem.* 36, 1143 (2006).
7. S. Mukerjee, S. Srinivasan, and M. P. Soriage, *J. Phys. Chem.* 99, 4577 (1995).
8. T. Toda, H. Igarashi, and M. Watanabe, *J. Electrochem. Soc.* 460, 256 (1999).
9. A. K. Shukla, M. Neergat, B. Parthasarathi, V. Jayaram, and M. S. Hedge, *J. Electroanal. Chem.* 504, 111 (2001).
10. H. Cheng and K. Scott, *J. Electroanal. Chem.* 596, 117 (2006).
11. L. Liu, J.-W. Lee, and B. N. Popov, *J. Power Sources* 162, 1099 (2006).
12. V. Raghuvver, A. Manthiram, and A. J. Bard, *Phys. Chem. B* 109, 22909 (2005).
13. L. Fernandez, V. Raghuvver, A. Manthiram, and A. J. Bard, *J. Am. Chem. Soc.* 127, 13100 (2005).
14. A. Walsh, J. L. Fernández, and A. J. Bard, *J. Electrochem. Soc.* 153, E99 (2006).
15. J. L. Fernandez, J. M. White, Y. Sun, W. Tang, G. Henkelman, and A. J. Bard, *Langmuir* 22, 10426 (2006).
16. John F. Moulder, Kenneth D. Bomben, Peter E. Sobol, William, and F. Stickle, *Handbook of X-ray Photoelectron Spectroscopy*, Physical Electronics (1995).
17. A. Bzowski and T. K. Sham, *Phys. Rev. B* 48, 7836 (1993).

Received: 7 June 2007. Accepted: 30 November 2007.